International Journal of Environmental Sciences
ISSN: 2229-7359
Vol. 11 No. 6, 2025
https://theaspd.com/index.php

Impact of Substrate Height on Resonant Frequency of a Sputtering-Printed 28 GHz Microstrip Monopole Antenna

Bello Abullahi Muhammad[1], Mohd Fadzil Ain[1], Mohd Nazri Mahmud[1], Mohd Zamir Pakhuruddin[2], Ahmadu Girgiri[1], Mohamad Faiz Mahamed Omar[3], and Abdullahi S. B. Mohammed[1]
[1]School of Electrical and Electronic Engineering, Universiti Sains Malaysia, Penang, Malaysia
[2]School of Physic, Universiti Sains Malaysia, Penang, Malaysia
[3]Collaborative Microelectronic Design Excellence Center, Universiti Sains Malaysia, Penang, Malaysia
[*] Corresponding author: eemfadzil@usm.my

Received: 01st May 2021
Revised: 04th June 2021
Accepted: 15th June 2021

Abstract: *This research article aimed to design a 28 GHz printable microstrip monopole antenna on a polyimide substrate with varying thicknesses. To investigate the impact of substrate thickness variation on the resonating frequency. And introduced a new fabrication technique. To employ regression modelling and analyze the data obtained from the simulation results. The article developed quadratic polynomial equations that investigated the relationship between substrate height, center frequency, and bandwidth. The proposed antenna was designed with a compact size of 6 x 4.5 x 0.2 mm³ and realizes a bandwidth of (23.24 GHz - 31.54 GHz) with a return loss of 37.48 dB and 94% radiation efficiency. The proposed nanotechnology sputtering printing technique offers an effective printing technique that produces many antennas in a single operation. These enable mass production within a short period, reduce manufacturing costs, and save time. It also allows the production of smaller-dimension antennas even at the nanoscale. The antenna prototype was successfully printed with effective conductivity and surface roughness using the novel sputtering technique. The antenna was tested and validated for millimeter-wave applications. The paper demonstrated the fundamental mechanisms for antenna designers, which gave insight into frequency sensitivity and millimeter-wave applications.*
Keywords: *Center frequency, Bandwidth, Polynomial equations, Sputtering technique, Substrate height.*

1. INTRODUCTION

In recent years, substrate height (hs) has become a challenging research topic in antenna design, as the thickness of the dielectric material separates the ground and the patch conductive layers. It is a component or parameter property that influences the shift in center frequency (F_C) and bandwidth (BW) (Alkhafaji et al., 2020). Substrate thickness affects the propagation of the electric field, impedance, distribution of electromagnetic waves, and overall efficiency in the antenna (Tütüncü and Kösem, 2022). Therefore, a change in hs can affect the effective wavelength and dielectric constant, resulting in a shift in the F_C and BW (Sarma et al., 2020). The substrate allows more energy storage within the dielectric materials, increasing the antenna wavelength. The frequency is inversely proportional to the antenna wavelength, and a thicker substrate produces an antenna with lower radiation efficiency (Sarma, 2020). High hs can increase losses and spurious radiation, negatively impacting antenna performance (Ramli et al., 2020).

A microstrip antenna with a thinner substrate has higher resonating frequencies, and a thicker substrate causes lower resonating frequencies due to a change in wave confinement (Muhammad et al., 2023). A thin substrate antenna has improved radiation efficiency for the sub-5G wireless application (M. Kim et al., 2022). A printed antenna on an ultra-thin flexible substrate of 25 micrometers (μm) has improved performance for Internet of Things applications (Wagih, 2020). A thin, flexible, and wearable printed antenna with a large bandwidth was produced and proposed for biomedical applications (Kumar et al., 2021). A microstrip antenna with various substrate thicknesses confirmed that a thicker substrate achieved better return loss and

lower gain, while a thinner substrate causes poor return loss with higher gain (OAhmed et al., 2022). Therefore, the choice of substrate thickness depends on the required performance factor and application.
Polyimide (PI) substrates have low dielectric permittivity, flexibility, and efficiency at high frequencies (Saleh et al., 2024). A PI with a micro-crosslinked and nanocomposite structure enhances circuitry integration by reducing the dielectric constant (Peng et al., 2024). Palladium ion reduction and free radicals to copolymerize 4-vinyl pyridine, enhancing catalyst adhesion and enabling a PI-based antenna for high-frequency applications (You et al., 2022). The thin PI-based antenna has been popular for ultrawideband (UWB) applications (Lukacs et al., 2022). A PI-based microstrip antenna has played a vital role in biomedical applications for pressure and level sensing under various temperatures (Sindhu et al., 2022). The PI-based microstrip antennas are of interest in industrial, science, and medical (ISM) frequency bands, among others (Ahmed et al., 2024). The high demand for antennas for such applications led to the choice of PI substrate in this research article. A fabricated, mm-wave and PI-based antenna design with a 0.1 mm thickness has been reported to be suitable for IoT and wearable applications (Shariff et al., 2024). A fabricated microstrip antenna on a thin PI substrate decreased antenna weight by up to 92% compared to conventional substrates (Tang et al., 2024). A thin, flexible PI-based monopole antenna with an enhanced bandwidth and higher radiation efficiency has been tested and validated for higher performance (Liu et al., 2022). Considering the impact of hs on the antenna performance in terms of BW and F_C, antenna designers should consider hs very important in the antenna design and optimization. The proposed work revealed the influence of hs on the performance of antennas for F_C, BW, and other parameters in mm-wave and frequency sensitivity applications. Thin PI substrate-based antennas are becoming popular due to their flexibility, low cost, low power consumption, and high performance.
Microstrip antennas have been a research topic for many years, with lightweight, low cost, simplicity in design and fabrication (Hirendra and Sharma, 2022). Thus, its counter limitations are narrow bandwidth, low gain, surface wave loss, and radiation efficiency (Xu, 2022). An appropriate choice of substrate and its thickness can address these challenges and improve the antenna's performance. The process of substrate height variation enables the right choice of a suitable substrate thickness. These will also overcome the challenges of radiation losses and dielectric losses. The new sputtering printing techniques and silver ink enhance the challenges of the printing process of the printed antenna.
Most studies do not conduct enough research on the effect of substrate thickness on the microstrip monopole antenna resonant frequency and bandwidth at higher frequencies. And most of the literature focuses on lower frequencies. Moreover, further research is required in high frequencies such as mm-wave and terahertz frequencies for 5G and beyond applications. The flexible polyimide substrate is more reliable for using metallic inks, offering a fast and accurate fabrication technique for low-cost and mass production.
Moreover, a technique that can fabricate antennas on a thin, flexible substrate using metallic conductors is highly desirable for simplicity, mass production, and low cost in fabricating antennas suitable for various fields, such as the Internet of Things (IoT) and wearable devices for healthcare applications. This research employed a novel nanotechnology sputtering method to fabricate the proposed antenna using conductive silver ink, which provides strong bonding, surface roughness, and uniformity of the conductive material, to overcome the outstanding challenges in the printing technologies of antennas.

2. METHOD

2.1 Antenna Design and Configuration

Many flexible substrates, including polyesters, textiles, and polymers with varying thicknesses and electrical properties, have emerged for the design and fabrication of printable antennas (Qureshi et al., 2024). Thus, a thinner substrate has been reported to be suitable for higher-frequency antennas due to its better radio frequency properties in high-speed communication applications (Le et al., 2024). A literature review on the impact of dielectric permittivity on microstrip antenna design revealed the effect of varying substrate thickness on the antenna, where an increase in the dielectric constant leads to a decrease in bandwidth and gain (Hassoun et al., 2022). Designing an antenna on a polymer substrate with a lower substrate thickness can attain good radiation efficiency for high-frequency applications. Typically, a thinner substrate offers good performance of a printable antenna at high frequencies (Alamdar et al., 2024). A study on the impact of substrate thickness on an antenna operating in mm-wave, shows that a substrate with a smaller dielectric constant of εr = 2.2, 3, or 4 realized an enhance bandwidth with an improved in gain, and a dielectric constant (εr = 10.2) gives an increase in the dielectric loss and surface wave loss (Ermıs, 2024).

The proposed monopole antenna comprises a PI substrate, a radiating silver patch element, a coplanar waveguide, and a feeding line, with the PI substrate thickness ranging from 0.100 mm to 0.75 mm. This variation of the substrate affects the antenna design and optimization process as well as the resonating frequency. Thus, understanding the relationship between the substrate thickness and the antenna parameters' performance is necessary before the design and optimization begin. To effectively design and optimize a microstrip monopole antenna, it is necessary to comprehend the design parameters and know their mathematically estimated values before finally implementing them. A definition of the antenna parameters is displayed in a separate section in this manuscript. The basic procedure in designing a microstrip monopole antenna includes selecting a suitable dielectric material, its dielectric constant value ε, loss tangent δ, and thickness.

A dielectric constant with a lower value was thought to attain a high resonant frequency and a narrow bandwidth. Consequently, in this research article, a thin substrate at a higher frequency, particularly in mm-wave, achieved a wider bandwidth than in other literature. Typically, a thicker substrate increases surface wave losses and impedance mismatch. The thicker substrate leads to a wider bandwidth; in some cases, a thinner substrate weakens the parting between the ground plane and the patch, which in turn decreases effective permittivity. A weaker effective permittivity enlarged the guide wavelength, reduced the quality factor of the resonator, causing an improvement in impedance matching, resulting in an increase in bandwidth for the microstrip monopole antenna.

The proposed design has confirmed that the substrate thickness resulted in surface wave loss, leading to weakened radiation efficiency and unwanted radiation patterns, which limit antenna performance. Moreover, a thin substrate causes a negligible surface wave excitation when a field is confined to the transmission mode in microstrip feedlines. The surface wave excitation leads to minor surface losses and enhances antenna efficiency at higher frequencies. As the substrate thickness increases, the more simply excited surface wave propagation leads to a higher surface wave loss, resulting in a reduced radiation efficiency and a power leakage. Thus, a thicker substrate alters the microstrip line characteristics and impedance matching, causes a mismatch, and affects the effective permittivity. Therefore, it is necessary to study and understand the impact of substrate thickness variation in the design and optimization processes for effective antenna performance.

The proposed 28 GHz microstrip monopole antenna employed an optimized coplanar waveguide (CPW) with a gap between the patch and feedline. It has a compact size of (6×4.5×0.2) mm^3. The antenna was designed and optimized with varying PI substrate height. Table 1 shows the dimensions, and Figure 1 illustrates the proposed 28 GHz printable microstrip monopole antenna design. Equation (1) demonstrates how to determine the width of the microstrip line, while a mathematical equation (2) calculates the height (hs) using the dielectric and conductive parameters. The equations (3) and (4) are regression equations.

$$w = \frac{7.48hs}{e(z_o \frac{\sqrt{\varepsilon_r + 1.4}}{87})} - 1.25Mt \quad (1)$$

$$hs = \frac{(w - 1.25Mt) \times e(z_o \frac{\sqrt{\varepsilon_r + 1.4}}{87})}{7.48} \quad (2)$$

Where Mt is the conductor thickness, Z_0 is the impedance, ε_r is the dielectric material, and hs is the substrate height.

International Journal of Environmental Sciences
ISSN: 2229-7359
Vol. 11 No. 6, 2025
https://theaspd.com/index.php

$$y = \beta_0 + \beta_1 x + \beta_2 x^2 + \ldots + \beta_n x^n + \varepsilon \quad (3)$$

$$\varepsilon = x\beta - y \quad (4)$$

$$\hat{\beta}_0 = \bar{y} - \hat{\beta}_1 \bar{x}$$

(5)

$$\hat{\beta}_1 = \frac{\sum_{i=1}^{n} (x_i - \bar{x})(y_i - \bar{y})}{\sum_{i}^{n} (x_{i=1}(x_1 - \bar{x})^2}$$

(6)

Where y is the response, x is the predictor, β_0 is the y-intercept, β is the regression coefficient, and ε is the random error.

Table 1: Dimensions of the proposed antenna designed

Parameter	*Dimension (mm)*	*Parameter*	*Dimension (mm)*
SL	6	W6	0.95
SW	4.5	W8	0.87
Mt	0.035	W9	0.2
hs	0.2	W10	1.26
Lf	3.28	L1	2.5
G1	0.35	L2	0.4
G2	0.25	L3	0.44
W1	0.7	L4&L7	1.98
W2&W7	0.3	L5	1.14
W3	0.47	L6	1.04
W4	0.23	L8	0.83
W5	0.3		

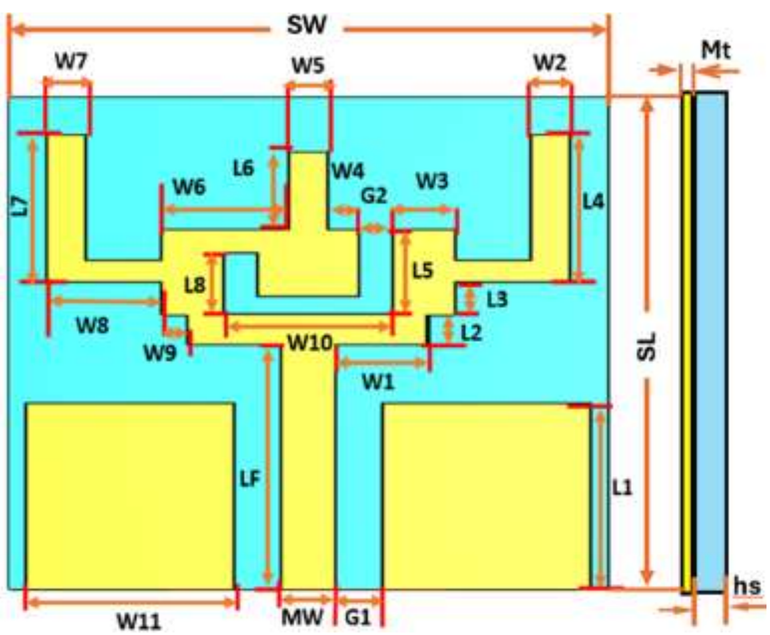

Figure 1: Proposed 28 GHz microstrip antenna design

2.2 Surface current distribution

The E-field is produced from the dielectric substrate properties and is strong through the edge of the patch due to the fringing effect. The fringing field primarily influences the radiation. The E-field distributed in one direction is responsible for distinct lobes in the antenna radiation pattern and reaches a maximum at the center of the patch, permitting the antenna to radiate.

The surface current flow is a crucial factor that shows the antenna; it determines the radiation pattern and polarization of the radiated electromagnetic wave. Figure 2 shows how the current flows and how it transmits electromagnetic waves in the proposed antenna. The current shows the radiation field direction, in which the current is high from the feedline and then decreases at the end of the patch. It flows between the antenna patch and the CPW and is not uniform, illustrating how the antenna radiation pattern propagates. The electric field distribution of the proposed antenna design at 28 GHz frequency and the surface current distribution of the proposed antenna illustrate that the majority of current flows from the feedline. The current flow at the CPW enhances the impedance matching of the antenna and increases the magnitude.

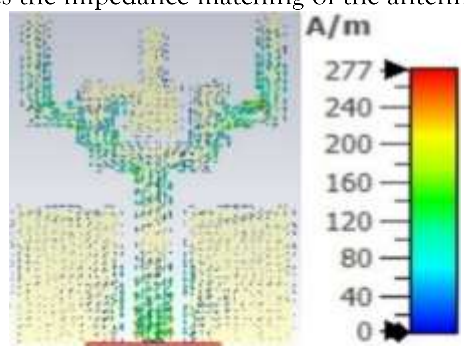

Figure 2: Current distribution at 28 GHz

3. FINDINGS AND DISCUSSIONS

1 Simulated Result

The proposed antenna realized a change in BW and shift in F_C; it achieved a BW of 8.30 GHz with a minimum return loss of 37.48 dB at 28 GHz. It displays a bidirectional radiation pattern with an average radiation efficiency of 94% and a peak gain of 3.76 dBi. It realized an increase in BW and F_C in a thinner. Table 2 shows the simulation result for various hs, resulting in different BW and shifts in the frequency response. Figure 3 illustrates the impact of the hs variation on the frequency response characteristic, including BW and F_C.

The results illustrate how the variation of hs affects impedance matching and eventually affects the BW. A lower hs sometimes enhances impedance matching and decreases effective permittivity. Increasing the guided wavelength has resulted in a reduction in the resonator strength, which leads to an improvement in the antenna's bandwidth.

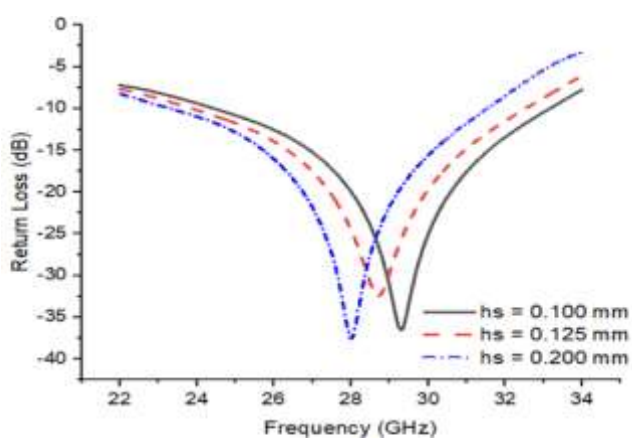

Figure 3: Impact of substrate height on center frequency and bandwidth

Table 2: Effect of substrate height on BW and F_C

Serial Number	*hs (mm)*	*Fc (GHz)*	*Operating band (GHz)*	*BW (GHz)*	*Percentage (%) BW*
1	0.100	29.370	23.87-32.54	8.67	29.52
2	0.125	28.780	23.84-32.48	8.64	30.02
3	0.150	28.336	23.54-32.03	8.49	29.96
4	0.175	28.000	23.39-31.70	8.31	29.68
5	0.200	28.000	23.24-31.54	8.30	29.64
6	0.225	26.908	22.96-28.50	5.54	20.59
7	0.250	25.756	22.90-27.33	4.43	17.20
8	0.275	25.516	22.86-27.09	4.23	16.58
9	0.300	25.312	22.75-26.88	4.13	16.32
10	0.325	25.108	22.59-26.68	4.09	16.16
11	0.350	24.940	22.42-26.48	4.06	16.28
12	0.375	24.552	22.44-26.06	3.62	14.74
13	0.400	24.465	22.39-25.98	3.59	14.62
14	0.425	24.280	22.32-25.57	3.25	13.39
15	0.450	24.081	22.28-25.27	2.99	12.42
16	0.475	23.994	22.23-24.89	2.66	11.09
17	0.500	23.706	22.19-24.51	2.32	9.79
18	0.525	23.521	22.14-24.37	2.23	9.48
19	0.550	23.414	22.09-24.14	2.05	8.76
20	0.750	23.284	22.02-23.98	1.96	8.42

4. Development of a regression model

The article developed the proposed model equations using the MINITAB software and the CST simulation results (data). The models were analyzed and evaluated for their fitness to the data. The proposed model equations provide accurate information for the prediction of antenna parameters, such as BW and F_C, and give information for the antenna design parameters. These assist in filtering design parameters to minimize the computational cost in the antenna design and optimization. Figure 3 (a) and (b) illustrate the regression model on the relationship between hs, BW, and F_C.

1. Proposed Developed Model Equations

The models were tested for the significance of terms to determine whether the final equation fits the data. The entire model equation chosen has testimony to the data and is substantial. Equation (7) shows the relationship between hs and BW, and equation (8) illustrates the relationship between hs and F_C. Table 3 summarizes the modes of fitness to the data, which satisfy the model significance and acceptability. Figures 4 (a) and (b) show the impact of hs on the BW and F_C on the proposed model equations.

$$BW = 12.35 - 33.24hs + 26.21hs^2 \quad (7)$$

$$F_C = 31.91 - 27.42\ hs + 21.53hs^2 \quad (8)$$

Table 3: Analysis of variance of the model

Model Fitness	*S*	*R-Sq*	*R-Sq(adj)*	*r*
BW	0.675	93.1%	92.2%	0.96
F_C	0.2968	97.9%	97.7%	0.99

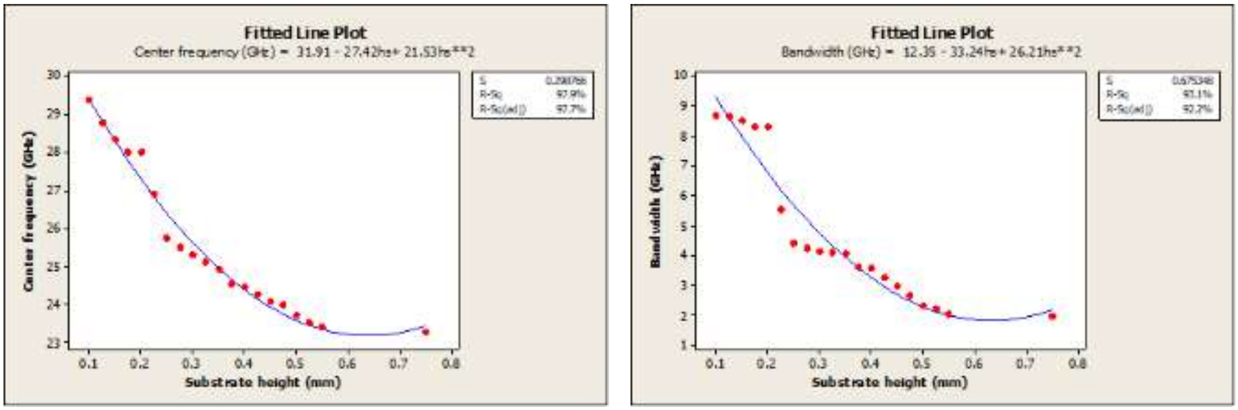

(a) hs vs Fc (b) hs versus BW

Figure 4 Impact of substrate height on center frequency and bandwidth

2. Analysis of variance of the proposed model

Analysis of variance (ANOVA) of the proposed models' equations, where BW and F_C are the response variables, while hs is the predictor. The model equations were analyzed using the results shown in the ANOVA table. The Table illustrates the performance of the proposed model equation to validate and signify its fitness and acceptability. We test the R-Square (R-sq) and R-sq adjust (R-Sq(adj) values to determine the model's fitness. R-sq and R-sq adjust (R-Sq(adj) closer to 1 indicate better model fitness and performance. The proposed model equation for BW R-sq is 93.1% (0.931), and R-sq(adj) is 92.2% (0.922), and for F_C, 97.9% (0.979), and R-sq(adj)is 97.7% (0.977). R-sq and R-sq(adj) values are closer to 1, which signifies a strong relationship between the model and the data. The correlation (r) between the hs and BW is 0.96, and the hs versus F_C is 0.99, signifying the model's strength. The acceptable p-values are between 0.000 and 0.050; the proposed model p-values for both BW and F_C are 0.000. In conclusion, the proposed models' equations are significant and acceptable. Tables 4 and 5 show the ANOVA of the proposed regression (Reg.) models. Equation (7) is the correlation between the data and the developed model, while equation (8) is the R-sq that calculates the model's fitness.

$$r = \sqrt{(R-sq)} \tag{7}$$

$$R-Sq = 1-\frac{SS_{Error}}{SS_{Total}} \tag{8}$$

Where r is the correlation, R-Sq is the R-square, SS_{Error} is the sum of the squares error, and SS_{Total} is the total sum of squares error.

Table 4: ANOVA of BW Vs hs

Source	*DF*	*SS*	*MS*	*F*
Regression	2	103.87	51.933	113.86
Residual Error	17	7.754	0.4561	
Total	19	111.62		

Table 5: ANOVA of F_C Vs hs

Source	*DF*	*SS*	*MS*	*F*
Regression	2	71.361	35.681	399.73
Residual Error	17	1.517	0.0893	
Total	19	57.788		

3. ANOVA of the residual plots and error behaviors

The article developed different models using the CST simulated data set provided, illustrating how the models fit into the data. The scatter diagrams were analyzed to choose the models that fit the data. It observed the variance of the residual values for each model, and then the model with the lowest variance of the residual values was chosen. Figures 5 (a) and (b) illustrate the residual plots and error behaviors of the fitted value for hs versus Fc and hs versus BW, respectively. The histogram shows more error on -0.5 for Figures 6 (a) and (b), indicating that the errors fall within the model error limit, testifying to the model's fitness and acceptability. The residual value versus data order mean is zero (0), which signifies the model's validity. The models' mean values are zero, realizing the model's significance.

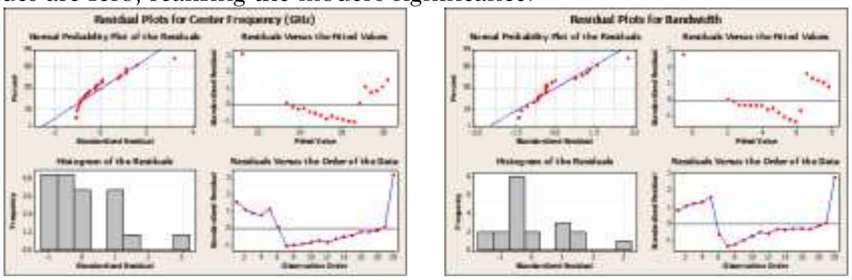

(a) BW versus hs (b) F_C versus hs

Figure 5: Residual plots as a function of fitted value: (a) BW versus hs and (b) F_C versus hs

5. FABRICATION AND MEASUREMENT RESULT

1. Fabrication Process

A novel and cost-effective fabrication technique utilizing a sputtering machine with silver ink, which is toxic-free and safe for skin and lungs, is employed to fabricate the proposed antenna, yielding better performance compared to inkjet printing technology. The fabrication process utilized a nanotechnology sputtering system, which deposited silver ink on the PI substrate within the sputtering chamber, thereby producing a printed area. The target material, which is the silver ink, was placed in the pumping chamber to deposit on the PI substrate and obtain the printhead area of the proposed antenna. The desired antenna's conductivity can be obtained through multiple layers of ink deposition.

The steps presented in the antenna fabrication provide a comprehensive outline of the process, where a nanotechnology sputtering technique using direct current (DC) magnetron sputtering is used to deposit the target material. This research demonstrated how a direct current (DC) affects the sputtering process used to deposit silver ink and fabricated the proposed antenna. The DC magnetron is responsible for chemical vapor deposition of the target material onto the desired substrate, in this case, the PI substrate, to print out the proposed antenna prototype. The PI substrate was cleaned to remove unwanted gases and impurities before the silver ink layers were deposited to print the proposed antenna, with surface roughness and conductivity. An argon atom was ionized under a higher DC voltage, enabling uniform silver layer deposition and conductivity. The target material was positioned in the sputtering chamber to remove unwanted gases. Then, the higher DC voltage was applied to the magnetron to trigger the argon atoms to be ionized and form a uniform conductive layer on the PI substrate. The process ensured strong bonding and good conductivity, and an appropriate surface roughness. The vapor deposition technique enhanced bonding capacity and desired electrical conductivity with surface roughness on the antenna prototype.

The technique of using the nanotechnology sputtering printing process provides an effective method to print many antennas in a single operation. The process enables mass production within a short period, significantly reduces manufacturing costs, and saves time. Furthermore, the accuracy of sputtering methods enables printing antennas in smaller dimensions, even at the nanoscale, and provides antennas for low-profile electronic devices and advanced communication systems. The advanced communication systems include wearable devices that require compact and high-performance. The silver ink properties, including surface tension, viscosity, adhesion, resistivity, and printability characteristics of an electrical impedance of less than 200 Ω, were confirmed when demonstrated on the thin, flexible PI substrate. Figure 6 shows the process of the proposed sputtering printing.

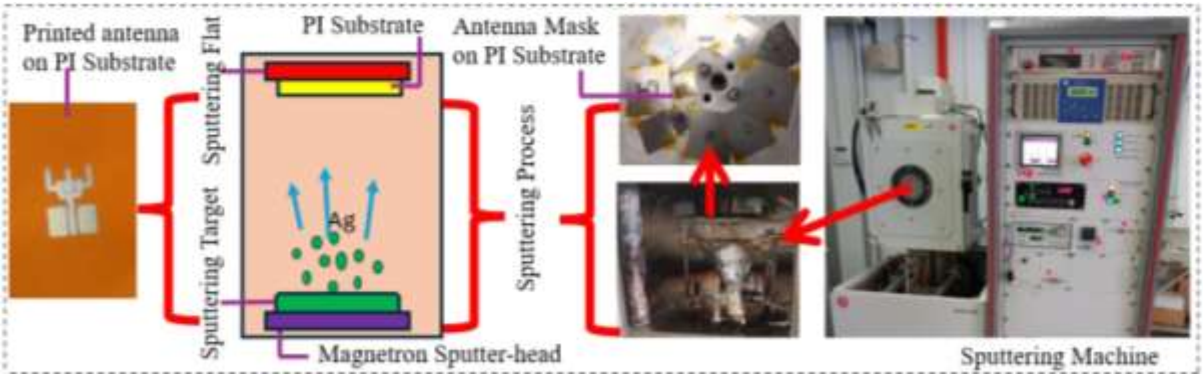

Figure 6: a proposed sputtering printing process with the sputtering machine

2. Lead-free Reflow

A solder paste is first heated to a molten state and used to connect the component to the target surface. The antenna is placed and heated into the MSA connector for reflow, and then the last stage is cooling the heated paste on the antenna prototypes. This work used conductive silver paste as solder paste. Figures 7 (a) and (b) show the antenna prototype with a lead-free reflow process technique.

(a) a lead-free reflow system (b) Antenna prototype

Figure 7: Lead-free Reflow Process

3. Measurement Setup

The process of the experiment and experimental setup to determine the radiation characteristics for the proposed antenna measurement and evaluation is conducted in an eco-friendly environment.

4. Return Loss

The measurement of the reflection coefficient was conducted immediately after the fabrication. A network analyzer measures the reflected signal in decibels (dB) of the proposed antenna and compares its result with the simulated result. The return loss measurement of the signal power reflected toward the source illustrates how the antenna radiates. The measurement result shows a variation due to impedance mismatch, illustrated in Figure 8 with the antenna prototype.

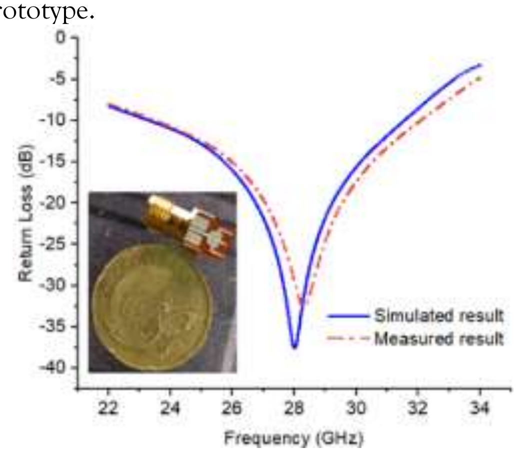

Figure 8: Return loss measured and simulated result with the antenna prototype

5. 2D radiation patterns

The 2D radiation shows the antenna radiation pattern, illustrating how the antenna radiates. It displays the field strength in two orthogonal planes: horizontal and vertical (elevation) planes. The result shows the maximum radiation for both the E-plane and H-plane. The E-plane and H-plane displayed radiation patterns similar to the simulated ones, with distortion due to the impedance mismatch between the simulated and fabricated antennas. The measurement was performed in an anechoic chamber and analyzed for the proposed application. Figures 9 (a) and (b) show the simulated and measured 2D radiation patterns for the H-plane and E-plane, respectively.

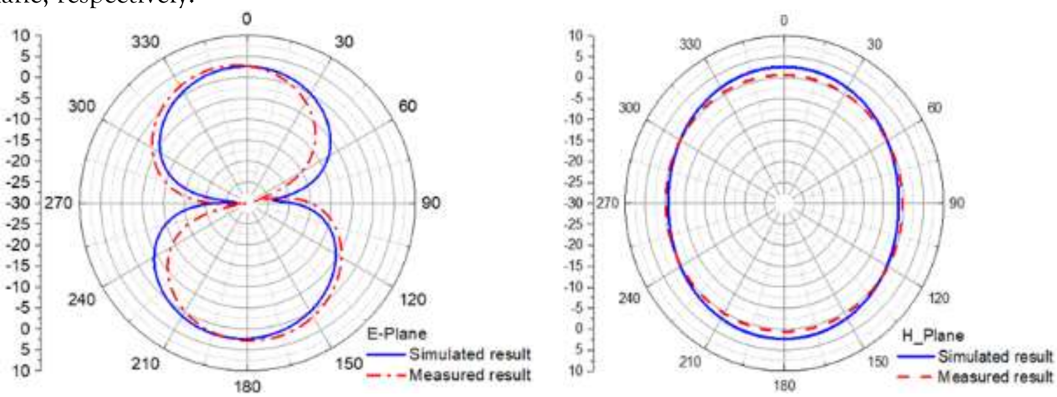

(a) H plane (b) H plane

Figure 9: 2D radiation patterns for simulated and measured results: (a) E plane, (b) H plane

6. Discussion

A prototype 28 GHz microstrip monopole antenna was designed and fabricated. The antenna was first simulated using CST Studio software and then measured with a network analyzer and an anechoic chamber. The E and H planes' radiation patterns experience a little distortion due to the impedance mismatch. The return loss was measured using a network analyzer and compared with the simulated result. The result was slightly disturbed due to the impedance mismatch. The paper also analyzed and evaluated the relationship between the hs and BW and F_C, discovering that the thicker the substrate, the lower the BW and F_C, while a thinner substrate attained higher BW and F_C values.

7. Comparative Analysis

Table 6 compares the proposed antenna's various parameters with those of other related works. This work achieved a wider bandwidth of 8.30 GHz and a high radiation efficiency of 94% using an appropriate substrate thickness. The proposed design has a compact size of 6×4.5×0.2 mm³ and achieves a better BW when compared with the other research work.

Table 6: A comparison between the proposed antenna and other related work

Ref.	*Fc (GHz)*	*Size (mm2)*	*hs (mm)*	*BW (GHz)*	*Gain (dBi)*	*Eff. (%)*
(C. M. Saleh et al., 2023)	28	12×12.8	0.508	6.00	5.00	95
(Awan et al., 2021)	28	2.5×4.5	0.203	6.40	5.62	87
(Zahra et al., 2021)	28	15×10	0.203	3.89	5.83	85
(Kumar et al., 2023)	28	5×3	1.6.00	4.41	4.49	89
(Elsharkawy et al., 2024)	28	5.5×12	0.254	6.10	5.00	88
This work	28	6×4.5	0.2	8.30	3.73	94

4. CONCLUSION

The proposed novel nanotechnology sputtering technique has fabricated a 28 GHz microstrip monopole antenna on a PI substrate using toxic-free silver ink, with the desired conductivity and surface roughness. The developed regression model equations analyze the relationship between the hs, F_C, and BW. The models have revealed the impact of the hs variation on the F_C and BW; thinner substrates achieved a wider BW, with a shift in Fc to a higher value, while thicker substrates reduced the F_C and BW values. The simulated and measured results are in good agreement, confirming the validity of the result and its suitability for the proposed mm-wave applications.

Acknowledgements
This work is supported by the Ministry of Higher Education Malaysia through the Fundamental Research Grant Scheme 218 under FRGS/1/2023/TKO7/USM/01/1.

REFERENCES

1. Ahmed, A., Li, D., Fan, Y., Li, R., Zhang, L., Qin, P., and Li, E.-P. Toroidal dipole metasurface based on polyimide substrate for flexible electronic applications. *IEEE Antennas Wirel Propag Lett*, 2024, 23, 1–5.
2. Ahmed, OlaF., Thaher, R. H., and Ahmed, S. R. Design and fabrication of UWB microstrip antenna on different substrates for wireless communication systems. *International Congress on Human-Computer Interaction, Optimization and Robotic Applications (HORA)*, 2022, 1–4.
3. Alamdar, S., Bagherkhani, S., De Flaviis, F., and Saadat, S. Millimeter wave dual-band antenna array on a thin flexible substrate for 5G applications. *United States National Committee of URSI National Radio Science Meeting (USNC-URSI NRSM)*, 2024. 61–62.
4. Alkhafaji, M. K., Alhamadani, H. A., Al-Yasir, Y. I. A., Saleh, A. L., Parchin, N. O., and Abd-Alhameed, R. A. Study on the effect of the substrate material type and thickness on the performance of the filtering antenna design. *Telkomnika (Telecommunication Computing Electronics and Control)*, 2020, *18*(1), 72-79.
5. Awan, W. A., Naqvi, S. I., Naqvi, A. H., Abbas, S. M., Zaidi, A., and Hussain, N. Design and Characterization of Wideband Printed Antenna Based on DGS for 28 GHz 5G Applications. *J Electromagn Eng Sci.*, 2021, *21*(3), 177-183.
6. Das Hirendra and Sharma, M. and X. Q. Microstrip antenna: an overview and its performance parameters. In J. and M. B. T. P. and K. G. and A. S. Malik Praveen Kumar and Lu (Ed.), *Smart Antennas: Latest Trends in Design and Application*. Springer International Publishing, 2022, 3–14.
7. Elsharkawy, R. R., Hussein, K. F. A., and Farahat, A. E. Miniaturized multi-band millimeter-wave vivaldi antenna with performance optimization at 28 GHz for 5G MIMO applications. *J Infrared Millim Terahertz Waves*, 2024, *45*, 3–4.
8. Ermıs, S. The effect of substrate dielectric constant and thickness on millimeter wave band patch antenna performance. *Celal Bayar Üniversitesi Fen Bilimleri Dergisi*, 2024, 20(4), 40–59.
9. Gatti, R. V., Rossi, R., and Dionigi, M. Single-layer line-fed broadband microstrip patch antenna on thin substrates. *Electronics (Switzerland)*, 2020, *10*(1). 1-14.
10. Hassoun, Z. A., Wali, M. H., Hussein, H. A., Haroon, N. H., and Alkhayyat, A. Study the effect of dielectric permittivity and changing substrate material on the microstrip patch antenna. *International Congress on Human-Computer Interaction, Optimization and Robotic Applications (HORA)*, 2022, 1–5.
11. Kim, J.-H., and Kim, B.-G. Effect of feed substrate thickness on the bandwidth and radiation characteristics of an aperture-coupled microstrip antenna with a high permittivity feed substrate. *J Electromagn Eng Sci.*, 2018, *18*(2), 101–107.
12. Kim, M., Lee, D., Oh, Y., Lee, J.-Y., Kim, B., Park, J., Park, D., and Hong, W. Antenna-on-display concept on an extremely thin substrate for sub-6 GHz wireless applications. *IEEE Transactions on Antennas and Propagation*, 2022, *70*(7), 5929–5934.
13. Kumar, P., Ali, T., Kumar, O. P., Vincent, S., Kumar, P., Nanjappa, Y., and Pathan, S. An ultra-compact 28 GHz arc-shaped millimeter-wave antenna for 5G application. *Micromachines*, 2023, *14*(1), 1-10.
14. Kumar, P., Ali, T., and Sharma, A. Flexible substrate-based printed wearable antennas for wireless body area networks medical applications (review). *Radioelectronics and Communications Systems*, 2021, *64*(7), 337–350.
15. Le, T. H., Kaiser, M. P., Koezegi, J.-M., Murugesan, K. S., Gerhold, L., Hichri, H., Oishi, R., Nakano, R., Ndip, I., and Schneider-Ramelow, M. Wideband antennas on thin-film packaging substrates for 140 GHz 6G applications. *IEEE 74th Electronic Components and Technology Conference (ECTC)*, 2024, 732–737.
16. Liu, Y., Wang, Z.-L., Cang, D.-Y., Gong, J.-S., and Qu, H.-W. A polyimide-based flexible monopole antenna. *J. Mater. Sci.: Mater. Electron.*, 2022, *33*(3), 1686–1702.
17. Lukacs, P., Pietrikova, A., Vehec, I., and Provazek, P. Influence of various technologies on the quality of ultra-wideband antenna on a polymeric substrate. *Polymers*, 2022, *14*(3), 1-16.
18. Muhammad, B. A., Ain, M. F., Mahmud, M. N., Girigiri, A., Mohammed, A. S. B., and Omar, M. F. M. Design of printable microstrip patch antenna on flexible substrate for medical applications. *2023 Innovations in Power and Advanced Computing Technologies (i-PACT)*, 2023, 1–7.
19. Peng, Z., Ye, A., Zhang, L., Li, X., Lian, C., and Li, C. Micro-crosslinked polyimide nanocomposites with low dielectric constant and low dielectric loss for microwave antenna with molecular dynamics. *Compos. Commun.*, 2024, *46*, 101804, 1-7.
20. Qureshi, S., Hanif, M., Jeoti, V., Stojanović, G. M., and Khan, M. T. Review of fabrication of SAW sensors on flexible substrates: Challenges and future. *Results Eng.*, 2024, *22*, 102323, 1-11.
21. Ramli, N., Noor, S. K., Khalifa, T. Ben, and Rahman, N. H. A. Design and performance analysis of different dielectric substrate based microstrip patch antenna for 5 G applications. *Int. J. Adv. Comput. Sci. Appl.*, 2020, (11)8, 77-83.

22. Saleh, C. M., Almajali, E., Jarndal, A., Yousaf, J., Alja'Afreh, S. S., and Amaya, R. E. Wideband 5G antenna gain enhancement using a compact single-layer millimeter wave metamaterial lens. *IEEE Access*, 2023, *11*, 14928–14942.
23. Saleh, S., Saeidi, T., Timmons, N., and Razzaz, F. A comprehensive review of recent methods for compactness and performance enhancement in 5G and 6G wearable antennas. *Alex. Eng. J.*, 2024, *95*, 132–163.
24. Sarma, Ch. A. Effect of ground etching, inset feed, and substrate height on elliptically shaped patch antenna. *International Journal of Emerging Trends in Engineering Research*, 2020, *8*(7), 3145-3149.
25. Shariff, B. G. P., Pathan, S., Mane, P. R., and Ali, T. Characteristic Mode analysis based on highly flexible antenna for millimeter wave wireless applications. *J. Infrared Millim. Terahertz Waves*, 2024, *45*(1), 1–26.
26. Sindhu, B., Adepu, V., Sahatiya, P., and Nandi, S. An MXene based flexible patch antenna for pressure and level sensing applications. *FlatChem*, 2022, *33*, 100367, 1-11.
27. Tang, R.-Z., Qu, S.-W., and Yang, S. (2024). Lightweight broadband phased array antenna based on ultra-thin polyimide film. *IEEE Antennas Wirel. Propag. Lett.*, 2022, 1–5.
28. Tütüncü, B., and Kösem, M. Substrate analysis on the design of wide-band antenna for sub-6 GHz 5G communication. *Wirel. Pers. Commun.*, 2022, *125*(2), 1523–1535.
29. Wagih, M. Direct-write dispenser printing for rapid antenna prototyping on thin flexible substrates. *14th European Conference on Antennas and Propagation (EuCAP)*, 2020, 1–4.
30. Xu, K. Broadband microstrip antenna overview. *Highl. Sci. Eng. Technol.*, 2022, *27*, 621–629.
31. You, J.-L., Chang, C.-P., Pu, N.-W., Chen, Y.-S., Wang, L.-H., Pan, K.-H., and Ger, M.-D. Electroless plating of a 5G copper antenna on polyimide patterned with laser-induced selective activation and curing of metal–organic catalyst. *Appl. Surf. Sci.* 2022, *599*, 153990, 1-12.
32. Zahra, H., Awan, W. A., Hussain, N., Abbas, S. M., and Mukhopadhyay, S. Helix inspired 28 GHz broadband antenna with end-fire radiation pattern. *Comput. Mater. Contin.*, 2021, *70*(1), 1933-1944.